Some Observations on Periodic and Transient Motions on MAV-Relevant Unsteady Aerodynamics

Michael V. OL

U.S. Air Force Research Laboratory, Air Vehicles Directorate, Bldg. 45, 2130 8th St., Wright-Patterson AFB, OH 45433-7542
e-mail: Michael.Ol@wpafb.af.mil

The aerodynamics of flapping wings is ultimately concerned with the relation between motion kinematics and the time-history of aerodynamic forces and moments. But an important intermediate quantity is the evolution of the flowfield – and in particular of flow separation. Nature's solution to large time-varying pressure gradients, for example those due to aggressive motions, is to form and eventually to shed vortices. We are interested in understanding and exploiting these vortices – for example, in delaying vortex shedding to promote lift in situations where flow separation is in any case inevitable. From the engineering viewpoint, the question is to what extent closed-form models and conventional numerical/analytical tools can estimate the aerodynamic force history, with an eye to eventually running large parameter studies and optimizations. We discuss several examples of computational-analytical-experimental comparison, with the emerging theme that often the prediction of aerodynamic force history is easier than resolving the underlying flowfield.

We outline several attempts to bridge from classical problems in unsteady aerodynamics, such as dynamic stall[1], to more topical questions in flapping-wings[2]. We consider four groups of unsteady aerodynamic problems: (1) moderate-frequency periodic sinusoidal oscillations of airfoils, 2D plates and low aspect ratio plates, in motions following classical problems of dynamic stall; (2) high frequency sinusoidal plunge and pitch of 2D airfoils, where pitch and plunge are compared in terms of lift coefficient history and the evolution of shed vortices; (3) transient high angle of attack pitch-up and return of airfoils and plates, where again lift coefficient history and flowfield evolution are compared; and (4) various motions of flat plates in hover, where the plate is free to orient itself in pitch, and there is tight coupling between vortex shedding and thrust production. We focus on Reynolds numbers in the range of 5,000 – 75,000, covering flapping-wing applications from large insects to medium birds. In all three cases the theme is computational-experimental synergy, looking for complementary strengths. For example, computations generally produce more refined data in boundary layers, especially for attached boundary layers right at the wall; whereas particle image velocimetry and other experimental methods can better track shed concentrations of vorticity as they travel far from the wall. But computations involving modeling can be easily led astray if the methodology from large Reynolds number, quasi-steady problems encountered in more traditional aeronautical engineering applications, is applied to flapping-wings. Computations, once validated and found to agree favorably with experiment, are powerful means for calculating the integrated aerodynamic coefficients, such as lift and pitching moment – which are notoriously difficult to measure experimentally. For high-rate unsteady experiments in air, inertial and structural effects are a problem, because physical motion rates must be large to achieve the desired dimensionless rates. Experiments in water solve the inertial but not the structural difficulties, because the physical motion rates are now fairly small, but apparent-mass effects greatly reduce the frequency response of the test article mounting scheme. We suggest as a working compromise the use of dye injection in water to preliminarily validate numerical predictions, and then use of computations for parameter studies, finally closing the loop with detailed quantitative velocimetry in experiments, once the computations have identified the most interesting cases.

For topic (1), accurate rendition of laminar to turbulent transition is important for proper computation of the flowfield, with similar consequences for facility flow quality on the

experimental side; that is, laminar flow assumptions can lead to spurious prediction of flow separation, and vice versa. However, at high effective angles of attack, separation becomes inevitable and effects of Reynolds number, boundary layer physics and so forth become far less acute. So we have the somewhat paradoxical conclusion that massively-separated problems are easier to compute than the more classical problems of attached flow. As an example, we consider a study of airfoil pitch-plunge and pure-plunge, with the former a moderate separation and the latter a deep dynamic stall case, with a strong leading edge vortex.

For topics (2) and (3), dimensionless rates and consequently pressure gradients are so large that neither transition nor geometric details such as airfoil sectional shape are of much significance. Instead, the so-called noncirculatory forces dominate, whenever acceleration is nonzero. To the extent surveyed, distinction between a nominally 2D model and one with aspect ratio = 2 are surprisingly small. There are indeed interesting spanwise variations due to low aspect ratio, but sectional views of vortex formation and evolution do not differ greatly. For the case of moderate-amplitude motion but high frequency, classical planar-wake approximations are entirely adequate for lift prediction, even for problems with strong vortex shedding and eminently nonplanar wakes. But of course, one's definition of adequate approximation is subjective. Departure from classical models to actual observations is just large enough that a comprehensive closed-form model remains elusive, even for simple geometries and abstracted flow problems.

For topic (4) we show only the available experimental results, comparing visualization of leading edge and trailing edge vortices for three types of hovering models: a nominally 2D translating plate, a moderate aspect ratio translating plate, and a flapping plate. All three show marked spanwise flow, but curiously the thrust coefficients in all cases are remarkably similar. It may generally be that case that very different flow separation and vortex formation modalities nevertheless evince a kind of convergence to similar aerodynamic coefficient histories. If this is indeed true, then this is good news for computations, as the requirements for detailed flowfield resolution become quite relaxed, if the objective is just to produce aerodynamic coefficient calculations for engineering purposes

1. Moderate-frequency periodic sinusoidal oscillations of airfoils, 2D plates and low aspect ratio plates

The models are a Selig SD7003 airfoil[3], nominally in 2D or spanning a water tunnel test section wall-to-wall; a flat plate of 2.5% thickness and round edges, also wall to wall; and finally, a flat plate of 2.5% thickness and aspect ratio 2.0, with round edges around its perimeter. The nominal Reynolds number of 60,000; a schematic of the airfoil side-view and photograph of the installation in a water tunnel are shown in Figure 1.

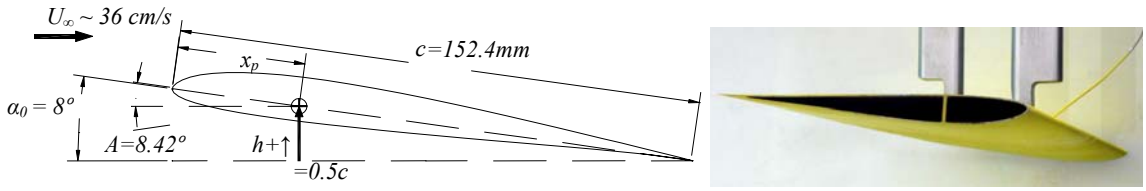

Figure 1. Schematic (left) and water tunnel installation (right) of SD7003 airfoil.

We consider the following kinematics for combined pitch and plunge, at a reduced frequency of 0.25, as shown in Figure 2 (reduced frequency $k = \pi fc/U_\infty$, c = airfoil chord and f = physical frequency):

$$\text{plunge: } h(t) = h_0\, c\cos(2\pi ft) = 0.5c\cos(0.5U_\infty t/c)$$

$$\text{pitch: } \alpha(t) = \alpha_0 + A\cos(2\pi(ft+\varphi)) = 8° + 8.42°\cos(0.5U_\infty t/c + \pi/2)$$

Pitch is about the quarter-chord, and leads plunge by a phase difference of 90°. Where pitch is zero, the resulting pure-plunge is a deep dynamic stall of peak effective angle of attack of around 22° (black curve in Figure 2). In the combined pitch-plunge case, the maximum effective angle

of attack is a shallower stall value of around 14° (blue curve in Figure 2). The plunge amplitude is 0.5 chords.

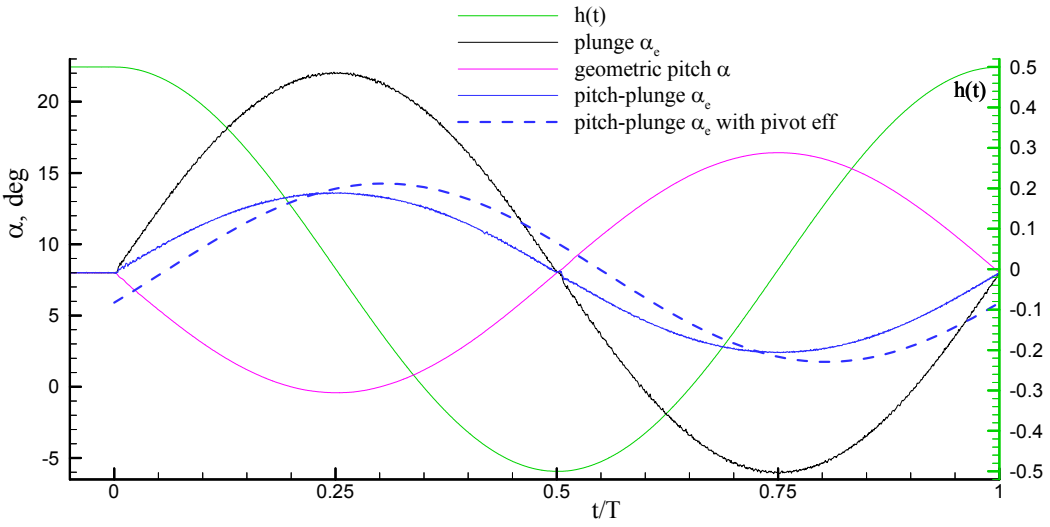

Figure 2. Time-traces of recorded angle of attack over one motion period, including start-up, for pure-plunge and pitch-plunge, k = 0.25.

The work reported here stems from an extensive computational and experimental campaign under the auspices of the NATO Research and Technology Organization, Applied Vehicle Technology Panel[4] For brevity the present discussion is limited to a handful of flowfield results, in the form of out-of-plane vorticity component contours, at the snapshot of halfway down the plunge downstroke, where effective angle of attack is maximum. Results for the pure-plunge case are given in Figure 3, and for the pitch-plunge case in Figure 4; both are for the airfoil.

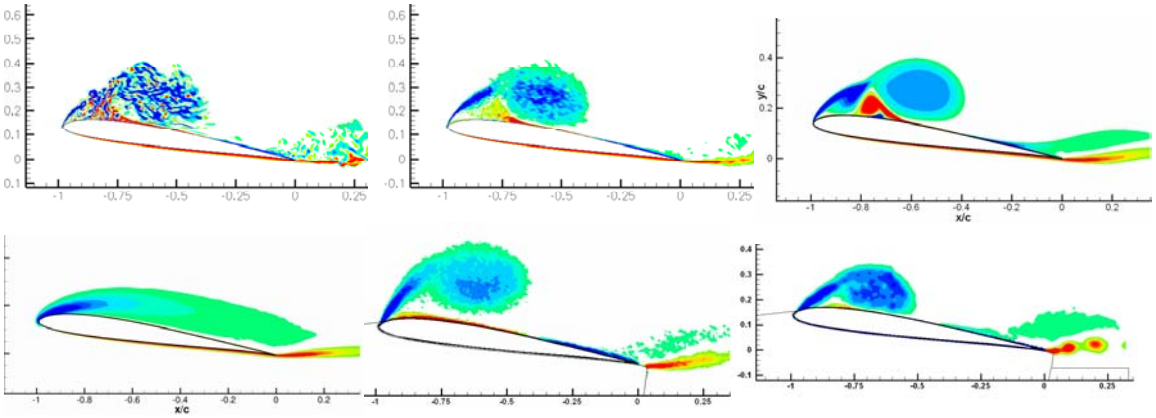

Figure 3. Contours of out-of-plane vorticity component for halfway down the plunge downstroke of the pure-plunge case, wall to wall SD7003 airfoil: Air Force Research Laboratory 3D Large Eddy Simulation (top left) and spanwise-average (top middle); Middle East Technical University Reynolds Average Navier-Stokes 2D computation (top right), University of Michigan 2D RANS computation (bottom left), AFRL particle image velocimetry in water (bottom middle), and University of Michigan PIV (bottom right).

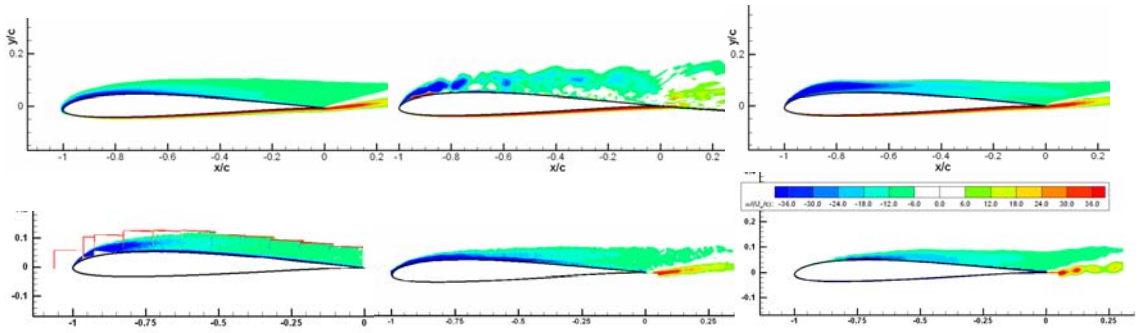

Figure 4. Contours of out-of-plane vorticity component for halfway down the plunge downstroke of the pure-plunge case, wall to wall SD7003 airfoil: University of Michigan 2D RANS (top left), Canadian National Research Council Institute for Aerospace Research 2D LES (middle top), METU RANS (top right), Technical University of Braunschweig wind tunnel PIV (bottom left), AFRL water tunnel PIV (middle bottom), and University of Michigan water tunnel PIV (bottom right).

The leading edge vortex (LEV) for the deep-stall case is quite evident in most of the results, while the shallow-stall is more of a quasi-steady separation. Paradoxically, the history of lift coefficient is easier to predict for the deep-stall case. This is because strong separation simplifies issues of transition, in computation and experiment alike. Figure 5 shows the scatter in lift prediction across a wide range of experiments and computations.

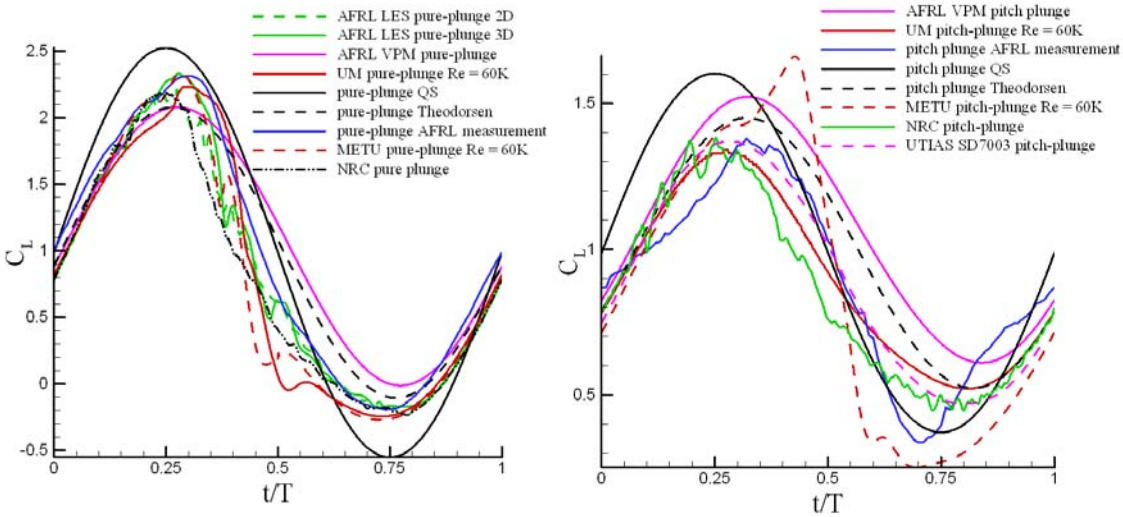

Figure 5. Lift coefficient history for the SD7003 airfoil, deep-stall case (left) and shallow-stall case (right), for various computational, analytical and phenomenological methods.

For the wall-to-wall plate with round edges, one would suspect that the sharper leading edge than that of the airfoil, and presumably the stronger leading edge pressure gradient, would result in less ambiguity in lift coefficient history prediction. As seen in Figure 5, this is true for the deep-stall case, but not for the shallow-stall case. For the latter, RANS computations overpredict LEV formation, and thus predict too high of a lift peak on the downstroke. The deep-stall case, on the other hand, is seen to be quite independent of cross-sectional shape – airfoil or plate.

Our final case in this section is the flat plate of aspect ratio 2, motivated by attempt to generalize from nominally 2D problems to insect-type of wings, and to classical problems in slender wing theory.

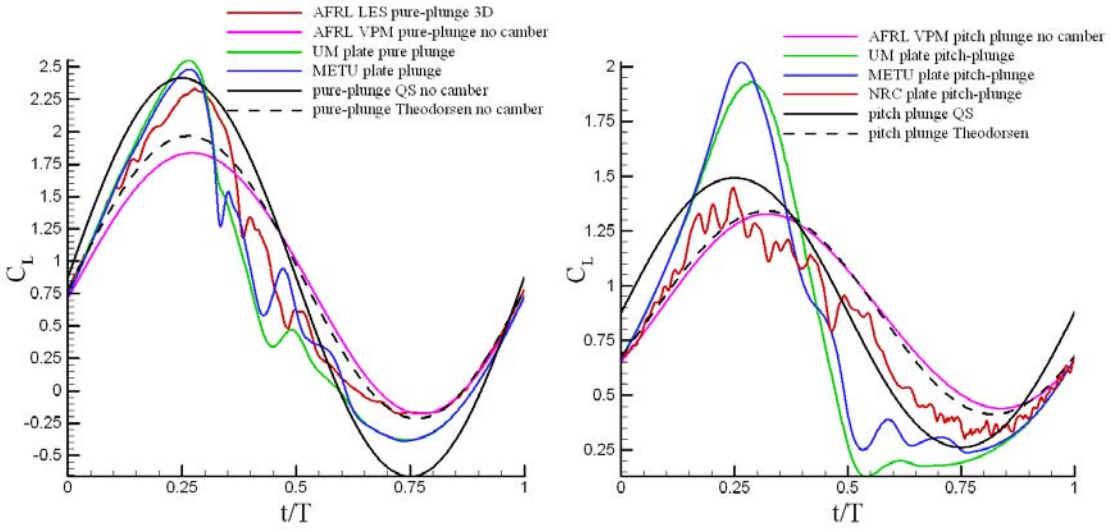

Figure 6. Lift coefficient history for the nominally 2D flat plate, deep-stall case (left) and shallow-stall case (right), for various computational, analytical and phenomenological methods.

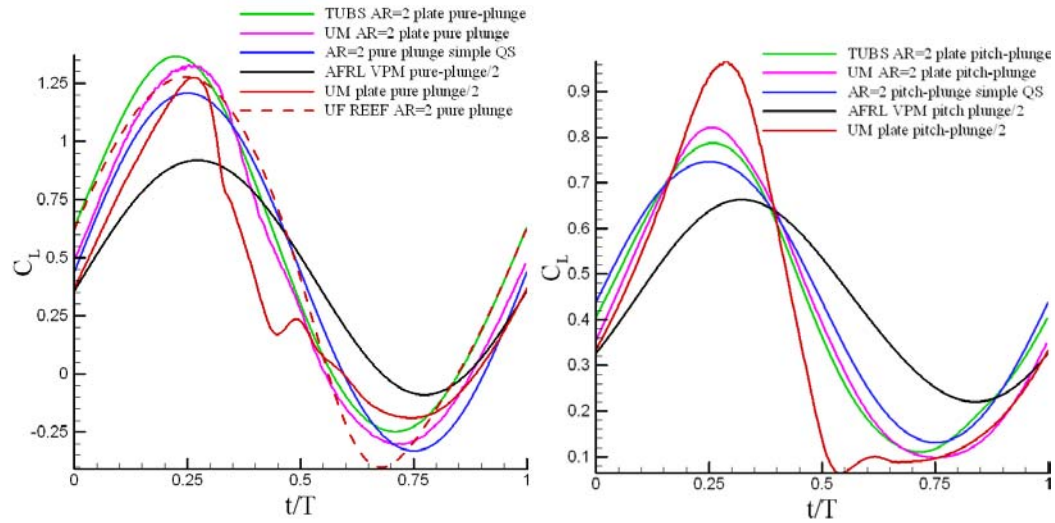

Figure 7. Lift coefficient history for the flat plate of aspect ratio 2, deep-stall case (left) and shallow-stall case (right), for various computational, analytical and experimental methods.

In sum, it is evident that RANS computations give acceptable accuracy in deep-stall problems which are not heavily influenced by boundary layer transition, but that transition-dominated problems likely require a higher level of sophistication, such as from 3D LES. Of course, it is likewise premature to claim that force measurement in experimental facilities, such as water tunnels, is a settled matter either. Perhaps the most surprising is the relative success of Theodorsen's method[5], despite the clear invalidation of its underlying assumptions in these flows. We next turn to a much higher reduced frequency and lower amplitude, where both computations and theory are much more successful.

2. High frequency sinusoidal plunge and pitch of 2D airfoils

The motion follows a large parameter study of small-amplitude high-frequency pure plunge by Platzer and Jones[6] on the NACA 0012 airfoil at zero incidence, motivated by application of flight propulsion by flapping wings. We focus on a high reduced frequency, k =

3.93. We are again using the SD7003, with a mean incidence of +4°, to produce mean nonzero lift. For low-amplitude high-frequency motion, flow separation is regularized by a small, concentrated and nearly wall-bounded LEV, which convects downstream along the airfoil suction side, at nearly the free-stream speed. Upon reaching the trailing edge, it merges into the wake, which for high enough Strouhal numbers will be a reverse Karman vortex street, indicative of a net thrust (propulsive) case, which in the stroke-averaged mean is a jet. At even higher Strouhal numbers, for plunge as well as pitch or combined motions, the wake becomes asymmetric, and the asymmetry is resolved in both experiment and computation; but that case will not be discussed here.

Figure 1. shows the normalized out-of-plane vorticity contours for the snapshot of halfway down the plunge downstroke, for k = 3.93, h = 0.05 plunge at Re = 40K, from a number of computations and an experiment. In sum, all results look much alike, and variation is much less than for low-frequency large-amplitude motions, evidently because the LEV formation process is largely independent of boundary layer transition physics, and because the formation process is largely two-dimensional. Even an inviscid vortex particle method calculates largely the same near-wake, despite its complete absence of an LEV model. Evidently, LEV-TEV interaction is not strong for this case.

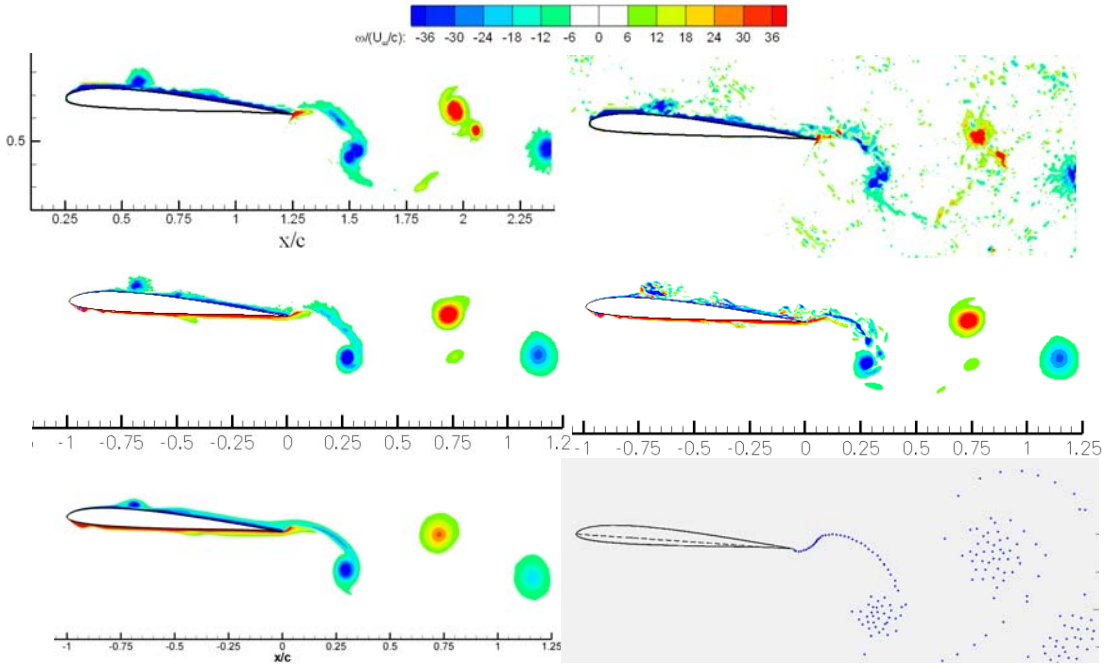

Figure 8. Contours of out-of-plane vorticity for SD7003 airfoil, k = 3.93 pure plunge: AFRL water tunnel PIV experiment, phase-averaged (top left) and instantaneous (top right); AFRL LES, phase averaged (middle left) and instantaneous (middle right); University of Michigan RANS (bottom left) and AFRL vortex particle method (bottom right).

Lift coefficient history is almost completely dominated by noncirculatory force, or apparent mass. In fact, Theodorsen's formula for lift coefficient is remarkably accurate for this case, despite the obvious fact that an LEV is present and the wake is not planar.

The success of Theodorsen's method suggests an exploration of the limits of linearity and superposition of solutions, and indeed a search for the limits of applicability of linear theory. One of the results of linear quasi-steady airfoil theory, and indeed of Theodorsen's method, is that for any prescribed airfoil pitching motion, one can solve for a plunging motion of the same lift coefficient history, and vice versa. A large set of pure-pitch, pure-plunge and combined pitch-

plunge cases was considered[7], of which we report one excerpt here. Quasi-steady airfoil theory predicts that the k = 3.93, h = 0.05 plunge has a lift coefficient history matched by a pure-pitch about the quarter-chord, with amplitude of 5.6 degrees and phase lead of 194.3 degrees. Therefore, a combined pitch-plunge motion, with pitch leading plunge by 14.3 degrees, should have cancellation of lift, and thus no lift variation with time. If instead Theodorsen's formula for lift coefficient is used, then the pitch history to cancel the plunge-induced lift is amplitude of 8.9 degrees and phase lead of 35.8 degrees. The results are shown in Figure 9, where dye injection from water tunnel experiment is compared with out-of-plane vorticity contours from a RANS computation (North Carolina State University[7]). While it is true that dye is a passive scalar and therefore is not a mathematically precise surrogate for vorticity, due concentration seems to compare well with vorticity contours whenever dissipation is low, as is presently the case.

Quasi-steady airfoil theory results in a pitch-plunge combination with very little concentrated vorticity resident in the near-wake, though there is still a small LEV. However, the lift coefficient variation is very much not zero. Entirely the opposite happens if instead we use Theodorsen's formula to arrive at the combination of pitch and plunge. That is, there is a vortex street, but the lift coefficient variation is only about 15% of the variation of either pure-pitch or pure-plunge. The conclusion is again about the dominance of noncirculatory lift; quasi-steady airfoil theory lacks a noncirculatory term, and therefore misses the lift coefficient history production. Theodorsen's formula does have a noncirculatory term, and performs reasonably well in lift coefficient prediction, even though its is inconsistent with the actual flowfield.

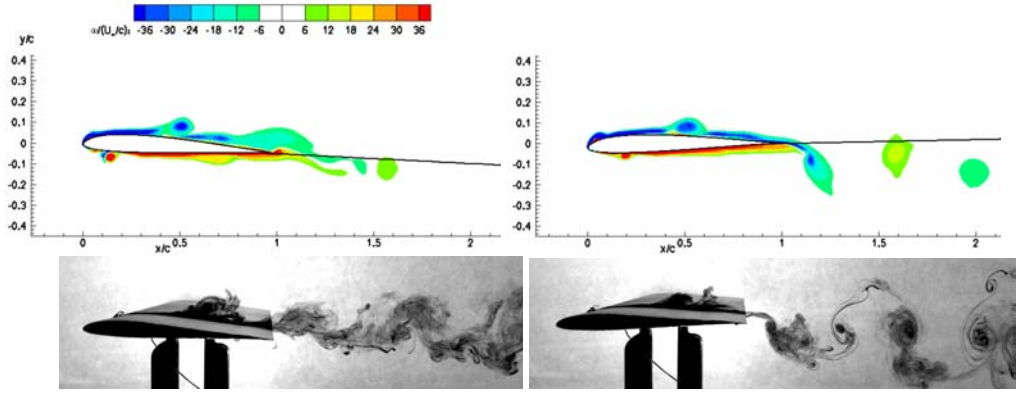

Figure 9. Dye injection (bottom row) vs. 2D RANS (top row), Re = 10K, SD7003 airfoil combined pitch and plunge, k = 3.93; combination based on quasi-steady airfoil theory (left), and Theodorsen's formula (right).

To summarize, low-amplitude high-frequency flows are relatively straightforward to compute and to resolve in water, and are reasonably amenable to attached-flow classical theoretical treatments. Lift coefficient history seems to be amenable to superposition, although the flowfield is not; speaking loosely, the lift history is more "linear" than the underlying flowfield. As the motion amplitude is increased, superposition becomes progressively less successful, and resolving the flow computationally becomes more complicated. We therefore next turn to an example of large-amplitude, high-frequency problems.

3. Transient high angle of attack pitch-up and return of airfoils and plates

Here we are interested in revisiting the classical problem of a 2D airfoil or plate executing a linear ramp motion in pitch, with a smoothing transient at motion onset and cessation. In the present case, the pitch is somewhat complicated by the addition of a brief hold at the maximum angle of attack, followed by a pitch-down to the original incidence angle, zero. Unlike the previously-examined cases, which were periodic, these are transient motions, where the

flowfield of interest is dominated by the effects of motion onset. Limiting the current discussion to lift coefficient time history, as opposed to flowfield evolution, the main objective is to again assess the role of circulatory vs. noncirculatory loads. Circulatory loads are due to shed and bound vorticity, while noncirculatory loads are due to acceleration, and can be calculated from inviscid analysis. And as with the low-amplitude periodic cases, we are interested in exploring the limits of superposition: can the two terms simply be added at high angles of attack and high motion rates? The answer is a qualified "yes". Noncirculatory effects are responsible for a spike in lift coefficient where motion acceleration is large, and go to zero where acceleration is zero. This can be seen from the lift coefficient trends in Figure 10, which compares two computations and a water tunnel measurement for a flat plate in sinusoidal and linear-ramp pitch. The dimensionless pitch rate is $K = c\dot{\theta}/2U_\infty = 0.20$. Interestingly, comparison between the three results is quite close, so the question becomes one of how to rationally construct a theoretical model. For the ramp, accelerations are limited to the "corners" of the angle of attack time trace, and these are the regions of time where lift has positive or negative spikes. Looking at the pitch upstroke, the noncirculatory lift contribution looks like a phase-lead to an otherwise quasi-steady lift response. But shortly before the top of the pitch upstroke, the lift response becomes more complicated, and superposition of circulatory and noncirculatory terms becomes speculative at best. We surmise that flow separation affects the noncirculatory calculation, and proper viscous treatment of noncirculatory lift may facilitate a partial rescue of separation. But in any case, the return-from-stall problem is much more complex than that of entry into stall.

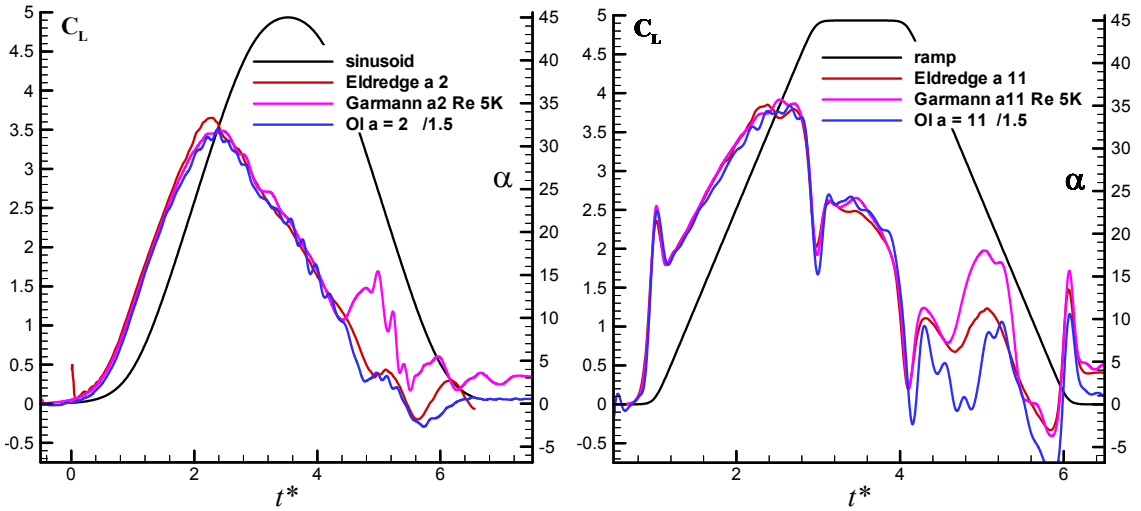

Figure 10. C_L for sinusoidal (left) and smoothed linear ramp (right) pitching motions of a flat plate with round edges and t/c = 0.025, from Garmann and Visbal computation (Re = 5000), Eldredge et al. computation (Re = 5000), and Ol et al. experiment (Re = 40,000)[8].

In our final set of cases, we take the limit of high reduced frequency to dispense with the free-stream completely, and consider the case of hover.

4. Free-to-pivot flat plates in hover: flapping vs. translation

In our final set of cases, we consider the problem of imposed sinusoidal motion in fore and aft translation, or up and down flapping (pivoting about a point near one wingtip). The second degree of freedom, pitch, is left unprescribed. The plate is hinged about its leading edge, such that it can rotate back and forth across 45° amplitude, with a mechanical limiter at either extreme. In the fore stroke, dynamic pressure from the imposed motion of the leading edge causes the plate to cling towards one angle of attack extreme. Near the limit of the imposed half-

stroke, the plate leaves its angle of incidence limiter, and rotates towards the opposite extreme. The process repeats on the opposite half-stroke. This is akin to "normal-hover"[9] with a peak incidence angle of 45°, except that in the usual normal-hover, the pitch trajectory is prescribed along with the plunge trajectory.

The overall objective is to explore the assertion that a flapping plate is fundamentally different from a translating plate, in that the former evinces retention of a leading edge vortex, but the latter sees leading edge vortex shedding shortly after formation. Presumably there should be a difference in thrust coefficient history as well. The secondary objective is to assess the role of aspect ratio, by comparing the wall-to-wall plate with one of aspect ration 3.4, following the geometry of a flapping-wing case proposed by Doman et al[10]. In brief, we find no significant difference in thrust coefficient history between the translating wall-to-wall plate, the translating AR=3.4 plate, and the flapping plate. Photographs of the configurations are given in Figure 11, and time traces of thrust coefficient for the three motions are given in Figure 12.

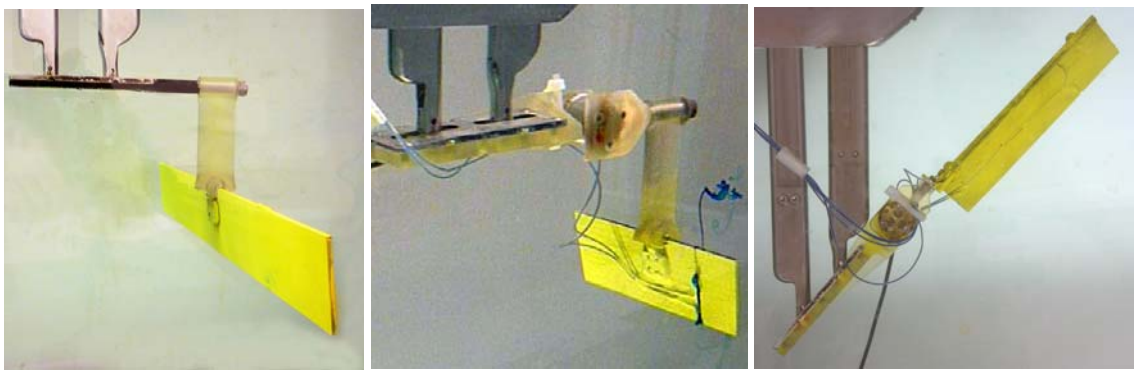

Figure 11. Free-to-pitch flat plates: translating wall-to-wall plate (left), translating AR=3.4 plate (middle), and flapping AR=3.4 plate (right).

All of the motions in Figure 12 evince spikes in thrust coefficient, but these are not noncirculatory spikes; they are simply from the free-to-pitch wing panel bouncing against the pitch limiter of the leading-edge hinge. The fore and aft strokes are nearly symmetric for the rectilinear cases. For the flapping case, there is a slight asymmetry due to buoyancy, since the wing is flapping in a vertical plane. Loosely speaking, all thrust coefficient responses are nearly sinusoidal, and are independent of Reynolds number over an approximate range of 5000 to 20000.

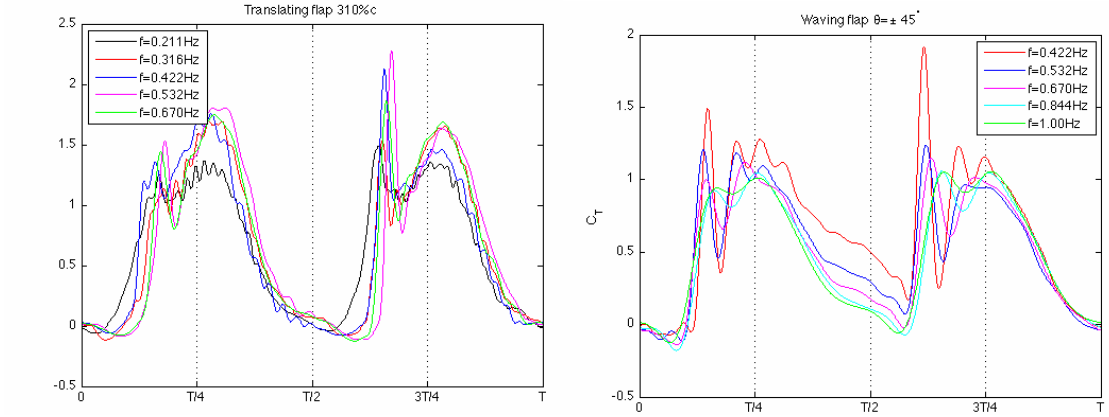

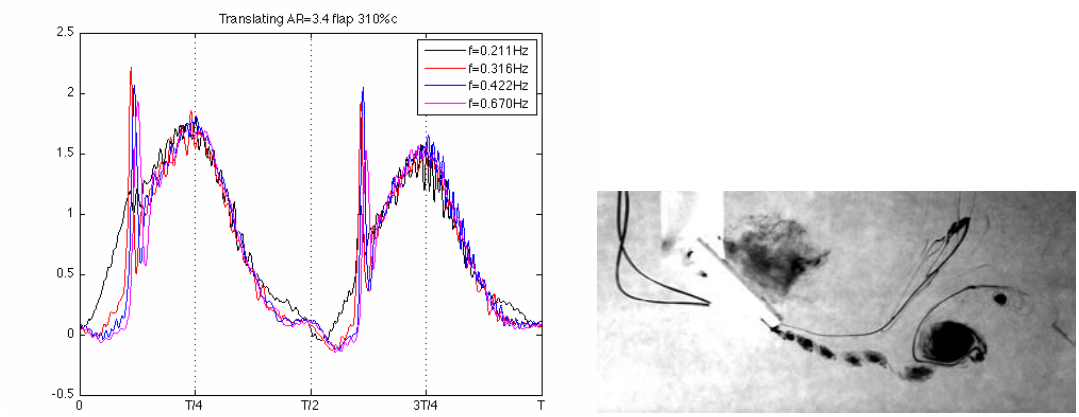

Figure 12. Thrust coefficient history for a range of Reynolds numbers, for a translating wall-to-wall plate (top left), flapping AR=3.4 plate (top right), and translating AR=3.4 plate (bottom left); typical vortex shedding process for translating AR=3.4 plate (bottom right).

Flowfields between the three motions do show their quintessential peculiarities, but as seen from the other cases reported above, aerodynamic force histories can be similar without flowfields necessarily being similar. As a corollary for computations, aerodynamic force can conceivably be predicted with good engineering accuracy, without necessarily full resolution of the flowfield physics. This is excellent news for Micro Air Vehicle designers. But as with all sweeping conclusions, much more work is required before we can substantiate an assertion as a truth.

Conclusion

Having considered several periodic cases and transient cases, we find that to a some extent, complicated details of the flowfield can be ignored in computational modeling, if the objective is calculation of lift coefficient. Even linear analytical models may be suitable predictors of lift, despite their underlying assumptions being falsified. The challenge is extending episodic observations to what begins to approach a universal theory, or at least a universal rule of approximation. For small-amplitude high-frequency motion, the problem is essentially already solved, but it remains to ascertain what one ought to mean by the limits of "small". Similarly, even in large-amplitude motions, there is potential for universal statements about the role of motion rates and displacements, in terms of their impact on flowfield development, and presumably lift as well. But this remains to be quantified. We recommend continuing the highly fruitful scheme of running "canonical problems" of well-defined geometries and motion conditions, to be executed by several different computations and experiments simultaneously. Only by duplication can we be assured of accuracy.

References

[1] Carr, L., "Progress in Analysis and Prediction of Dynamic Stall," *J. Aircraft*, Vol., 25, 1988, pp. 6-17.
[2] Dickinson, M. H., and Götz, K. G., "Unsteady Aerodynamic Performance of Model Wings at Low Reynolds Numbers," Journal of Experimental Biology, Vol. 174, Jan. 1993, pp. 45-64.
[3] http://www.ae.uiuc.edu/m-selig/ads/coord_database.html
[4] Ol, M.V. [ed.] NATO RTO AVT-149 Final Report, "Unsteady Aerodynamics for Micro Air Vehicles. Currently in-press.
[5] Leishman, J.G. *Principles of Helicopter Aerodynamics*. Cambridge University Press, 2000.
[6] Platzer, M., and Jones, K. "Flapping Wing Aerodynamics - Progress and Challenges" AIAA-2006-0500.

[7] McGowan, G., Gopalarathnam, A., OL. M.V., and Edwards, J. "Analytical, Computational, and Experimental Investigations of Equivalence Between Pitch and Plunge Motions for Airfoils at Low Reynolds Numbers". AIAA-2009-535

[8] OL, M., Altman, A., Eldredge, J., Garmann, D., and Lian, Y. "Summary of Progress on Pitching Plates: Canonical Problems in Low-Re Unsteady Aerodynamics". AIAA-2010-1085

[9] Shyy, W., Berg, M. and Ljungqvist, D. (1999) Flapping and flexible wings for biological and micro air vehicles. Progress in Aerospace Sciences, Vol. 35, pp 455-505.

[10] Doman, D., Oppenheimer, M., Bolender, M., and Sigthorsson, D. "Altitude Control of a Single Degree of Freedom Flapping Wing Micro Air Vehicle". AIAA-2009-6159